Processing and properties of PLA-HA nanocomposites: the effect of particle morphology and dispersants

Magdalena M. Tomczynska [a], Michael Ward[a], Gabriel Y. H. Choong[a], Kirsty Walton[a], Davide S. A. De Focatiis[a], David M. Grant[a], Derek J. Irvine[a] and Andrew J. Parsons[a*]

[a]*Faculty of Engineering, University of Nottingham, Nottingham, NG7 2RD, UK*

Magdalena.Tomczynska@nottingham.ac.uk

[*]*Andrew.Parsons@nottingham.ac.uk*

Abstract: Biodegradable polylactic acid nanocomposites for orthopaedic implants require optimum particle dispersion and high molecular weight in load bearing applications. Novel coated hydroxyapatite nanoparticles can offer new opportunities for enhanced dispersion during melt compounding. Nanocomposites compounded with a Minilab recirculating twin screw extruder have improved flexural strength when compared to the pure polymer. Dispersion of particles within the matrix was determined from transmission electron micrographs. Chromatography revealed that the polymer matrix of nanocomposites compounded over dry nitrogen had a higher molecular weight than that over air, and hence should exhibit delayed degradation within the body.

Keywords: Polylactic acid, nanocomposites, hydroxyapatite, melt compounding, TEM, GPC, flexural strength.
PACS: 81.05.Qk, 81.20.Hy, 83.50.Xa.

INTRODUCTION

Biodegradable polymeric implants are desirable alternatives to metallic orthopaedic implants such as screws and plates. Advantages include a reduction in stress shielding, radio-opacity and elimination of the requirement for a secondary removal operation, as their biodegradation products are extracted by natural metabolic pathways. An excellent candidate for biomedical applications is high molecular weight polylactic acid (PLA), which is a commercially available biodegradable polyester currently used for maxillofacial restorations, suture anchors and small screws. However, for load bearing conditions PLA requires reinforcement to match bone properties (cancellous bone: compressive strength between 2-20 MPa and elastic modulus between 0.1-2 GPa; cortical bone: compressive strength 100-200 MPa and elastic modulus 7-25 GPa) [1, 2].

Hydroxyapatite (HA), a natural constituent of bone, is favourable bioresorbable filler for PLA. Novel nano-sized hydroxyapatite particles (HANP) produced at Nottingham offer the opportunity to create resorbable nanocomposites with properties closer to those of bone. However, these properties depend on an optimum HA dispersion, which is challenging to achieve. Our previous work [3] introduced PLA-HA nanocomposites that made use of tailored HANP coatings to aid dispersion during melt compounding. This study investigates the effectiveness of these novel tailored dispersants on particle dispersion, melt properties and on macroscopic mechanical properties.

MATERIALS AND METHODS

Resomer LR706S - Poly(L-co-D,L-lactide) (PLDLLA) was supplied by Evonik Industries AG with a molar mass M_w of 445.9 kDa [4]. HANP with platelet and rod morphologies were synthesised via a hydrothermal counter-flow process [5 - 7] with dispersant coatings added in-situ [8, 9]. Post-production they were freeze-dried and stored in a dry anaerobic glove box. For dispersion, neat dodecenylsuccinic anhydride (DDSA) was purchased, whilst short-chained PLA with an isosorbide head group (is-PLA) [8, 9] and star shaped PLA 3 kDa (star-PLA) were polymerised via a standard ring-opening route involving lactide, a tin catalyst [10] and an isosorbide initiator. Nanoparticles were functionalised with dispersants with varying efficiency producing coated HANP with 50 wt% is-PLA8, 10 wt % DDSA, 30 wt% HANP is-PLA16, 35 wt% HANP star-PLA and 55 wt% HANP is-PLA24, measured via thermogravimetric measurements (TGA).

Nanocomposites were produced in a twin-screw recirculating extruder HAAKE MiniLab II fitted with co-rotating conical screws. Two pressure transducers in the recirculation channel provided pressure difference measurements used to determine the wall shear stress (τ_w). Materials were compounded at 210 °C with a screw speed of 50 rpm for 15 min in ambient air (Air) or in bottled nitrogen (N_2) at 1 bar and a flow rate of 0.3 l min^{-1} which was in-line dried (N_2D) with a liquid nitrogen moisture trap to remove residual water.

Proceedings of PPS-32
AIP Conf. Proc. 1914, 150004-1–150004-5; https://doi.org/10.1063/1.5016781
Published by AIP Publishing. 978-0-7354-1606-2/$30.00

Prior to compounding, PLDLLA was dried at 50 ºC under vacuum for a minimum of 8 hours to remove residual moisture, since water causes excessive hydrolysis during melt processing [11]. HANP were additionally dried for compounding in nitrogen: coated platelet HANP at 50 ºC under vacuum for 2 hours and neat HANP at 300 ºC in conventional oven for a minimum of 8 hours. Dried materials were transferred directly to the MiniLab compounder.

After extrusion, the molecular weights of neat polymer and nanocomposites were analysed using size-exclusion chromatography (SEC) in tetrahydrofuran (THF), calibrated with polystyrene standards. The viscosity average molecular weight (M_v) was used to describe the molecular weight of the nanocomposites:

$$M_v = \left[\frac{\sum M_i^{1+a} N_i}{\sum M_i N_i} \right]^{\frac{1}{a}} \quad (1)$$

where N_i is the number of moles of each polymer species of molar mass M_i and $a = 0.736$ [12] is the Mark–Houwink exponent for PLA in THF, relating the intrinsic viscosity to molar mass.

TGA tests were performed to confirm the HANP content for all the HANP-PLDLLA extrudates and the neat PLDLLA using a TA Instrument TGA Discovery, with a nitrogen purge gas flowing at 40 ml min^{-1}. Materials were heated up at 5 °C min^{-1} up to 500 °C and burned off isothermally for 20 min at 500 °C. Results were normalised by subtraction of the residual ash mass of neat PLDLLA.

A Transmission Electron Microscope, FEI TECNAI G2 BioTWIN with tungsten filament gun at an accelerating voltage of 100 kV (TEM FEI) was used to investigate the nanocomposite morphology directly after extrusion. Sections ~100 nm thick were cut using a glass knife and supported on copper grids.

For mechanical testing, the extrudates obtained from the MiniLab were compression moulded (CM) at 170 °C for 15 minutes to manufacture isotropic specimens subsequently used to produce minibars. Mechanical tests were carried out using an in-house miniature 3-point bending rig with specimen sizes of 7 x 2 x 0.5 mm. The initially produced air extrudates were injection moulded (IM) directly after compounding, with a HAAKE MiniJet injection moulding machine at 205 ºC with 800 bar pressure and a mould at 45 ºC. In an attempt to reduce the degree of polymer degradation, the injection moulding step was subsequently removed.

RESULTS AND DISCUSSION

TABLE (1). HANP- PLDLLA nanocomposites and PLDLLA recirculated in MiniLab in Air or N_2D. Summary of: HANP and coating wt% versus nominal loading; viscosity average molar mass M_v; wall shear stress τ_w, after 15 minutes recirculation; flexural strength σ measured on moulded bars.
[a]TGA wt% results; [b]wt% of coating in nanocomposite; [c]IM; [d]CM. Values are listed in ascending order of M_v.

Sample Name	Gas	HANP[a] [wt%]	Coating[b] [wt%]	M_v [kDa]	τ_w [kPa]	σ [MPa]
(1) 10 wt% HANP	Air	8.75 ±0.03	-	101.6 ±1.8	7.3 ±0.1	n/a
(2) 4.9 wt% HANP is-PLA8	Air	1.72 ±0.07	1.72	117.4 ±0.7	69.9 ±4.7	94.3 ±1.2[c+d]
(3) 2.8 wt % HANP DDSA	Air	2.37 ±0.04	0.26	121.8 ±1.1	66.7 ±3.8	n/a
(4) 5 wt% HANP	Air	4.42 ±0.04	-	150.8 ±2.6[c]	23.6 ±0.2	131.3 ±10.9[c+d]
(5) 3.6 wt% HANP is-PLA16	Air	2.38 ±0.08	1.02	175.5 ±1.2	49.8 ±0.4	n/a
(6) 2.5 wt% HANP	Air	2.29 ±0.16	-	181.6 ±2.0	44.0 ±0.2	83.6 ±3.0[d]
(7) 11.1 wt% HANP is-PLA24	N_2D	4.84 ±0.03	5.92	184.3 ±3.6	42.0 ±0.4	n/a
(8) 5.6 wt% HANP DDSA	N_2D	5.08 ±0.10	0.56	192.7 ±3.2	45.2 ±0.3	n/a
(9) 7.7 wt% HANP star-PLA	N_2D	4.70 ±0.09	2.53	193.3 ±1.2	43.0 ±0.3	n/a
(10) PLDLLA	Air	-	-	193.8 ±4.2	55.0 ±1.6	n/a
(11) 5.6 wt% HANP is-PLA24	Air	2.38 ±0.08	2.91	201.2 ±4.7	44.4 ±0.4	91.3 ±2.4[d]
(12) 3.9 wt% HANP star-PLA	Air	2.42 ±0.05	1.30	202.6 ±2.7	46.8 ±0.2	92.8 ±1.6[d]
(13) 2.5 wt% HANP rod	Air	2.50 ±0.09	-	206.8 ±2.8	60.8 ±3.4	92.0 ±3.9[d]
(14) 1 wt% HANP	Air	0.99 ±0.07	-	216.0 ±4.0	57.7 ±3.1	n/a
(15) 7.2 wt% HANP is-PLA16	N_2D	3.86 ±0.01	1.65	232.8 ±6.0	58.6 ±0.3	n/a
(16) 2.8 wt% HANP DDSA	N_2D	2.60 ±0.09	0.29	271.6 ±5.0	75.6 ±2.4	n/a
(17) 5 wt% HANP	N_2D	4.94 ±0.01	-	274.1 ±7.4	81.4 ±3.5	98.5 ±2.9[d]
(18) 3.9 wt% HANP star-PLA	N_2D	2.43 ±0.07	1.31	281.9 ±5.5	76.3 ±2.2	99.6 ±2.8[d]
(19) 5.6 wt% HANP is-PLA24	N_2D	2.48 ±0.09	3.03	288.6 ±3.9	79.1 ±4.8	92.7 ±2.6[d]
(20) 3.6 wt% HANP is-PLA16	N_2D	1.89 ±0.02	0.81	304.0 ±4.7	88.5 ±4.9	n/a
(21) PLDLLA	N_2D	-	-	309.0 ±4.0	85.0 ±7.1	91.7 ±4.5[d]
(22) 2.5 wt% HANP	N_2D	2.40 ±0.08	-	343.7 ±3.7	106.6 ±4.3	96.6 ±3.4[d]

Table 1 summarises all measurements on nanocomposites and PLDLLA recirculated in the MiniLab for 15 min in Air or N_2D. Sample names include the nominal total amount of coated or uncoated HANP compounded with PLDLLA. TGA results provide the final values of HANP wt% in the composite and coating wt% is calculated in relation to this, based on TGA tests performed on particles directly after coating. Additionally, τ_w after 15 min of recirculation in the MiniLab is recorded along with the flexural strength (σ) measured on bars produced via IM and CM, or CM alone. M_v of PLDLLA recirculated in N_2D is 37 % higher than in Air and M_v of nanocomposites compounded in N_2D is higher when compared to the nanocomposites in Air with the same nominal loading.

Figure 1 (a) shows a selection of data to illustrate the effect of HANP morphology and dispersant coatings on τ_w during processing in Air. A significant 55 % decrease in τ_w occurs due to PLDLLA degradation during 15 minutes of compounding, which causes reductions in molecular weight. HANP DDSA and HANP rod yield the highest τ_w, which may imply that more work is done in achieving a better dispersion.

Figure 1 (b) illustrates the importance of carefully drying nitrogen when it is used as an inert gas for melt processing of PLDLLA. This prevents excessive decrease of molecular weight caused by the presence of water, which can be a significant contaminant in bottled gas, and in result considerably mitigates reduction in τ_w during compounding. After recirculation in N_2 that has not been dried, τ_w is much lower than for either N_2D (58 % less) or Air (35 % less). Additionally, τ_w for Air decreases at a greater rate than for N_2D, inferring faster degradation causing an eventual larger decrease in molecular weight.

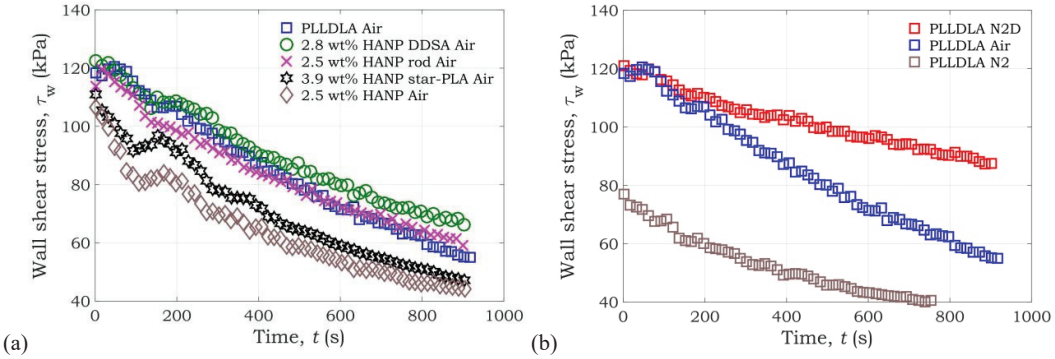

FIGURE 1. (a) Comparison of melt compounding of selected PLDLLA nanocomposites in Air with nominal loading of 2.5 wt% HANP. (b) Influence of moisture on melt compounding. All data filtered with moving average of 5 points.

Figure 2 (a) and (b) show the N_2D measurements of τ_w as a function of compounding time for a selection of nanocomposites from Table 1. The addition of 5 wt% HANP to PLDLLA in comparison to 2.5 wt% HANP leads to a significant decrease in τ_w, e.g. for HANP star-PLA τ_w reduced by 44 % after increasing the amount of HANP, probably indicative of inferior HANP dispersion or a plasticising effect of the particle coating. Additionally, the decreased gradient on Figure 2 (a) when compared to Figure 1 (a) confirms that residual moisture removal from N_2 is essential and drying HANP directly before compounding is beneficial.

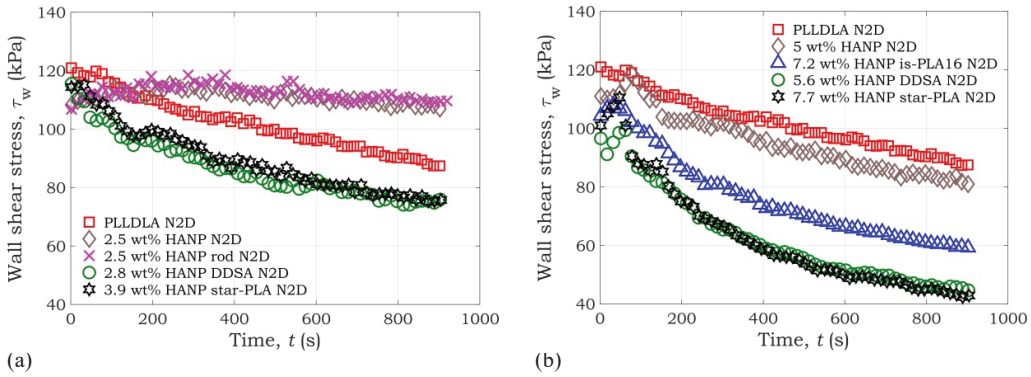

FIGURE 2. Comparison of melt compounding of selected PLDLLA nanocomposites in N_2D: (a) with nominal loading of 2.5 wt% HANP, (b) with nominal loading of 5 wt% HANP. All data filtered with a moving average of 5 points.

TEM images comparing selected nanocomposites from Table 1 compounded in Air and N_2D are shown in Figure 3. A simple method was employed for image analysis, determining the largest open square that can be applied on the image without crossing or encapsulating any particle [13]. This is a useful semi-quantitative

approach as it is assumed that the dispersion worsens with increasing free space. Dispersion of (i) 2.5 wt% HANP looks similar regardless of Air or N_2D compounding. (ii) 2.8 wt% HANP DDSA displayed superior dispersion in Air, which is in agreement with the compounding curve in Figure 1 (a), and (iii) 3.9 wt% HANP star-PLA appears enhanced in N_2D, which is in line with its τ_w in Figure 2 (a) when compared with Figure 1 (a). Applying the aforementioned image analysis method to Figure 3 reveals the greatest dispersion for 2.8 wt% HANP DDSA in Air in comparison to the other nanocomposites.

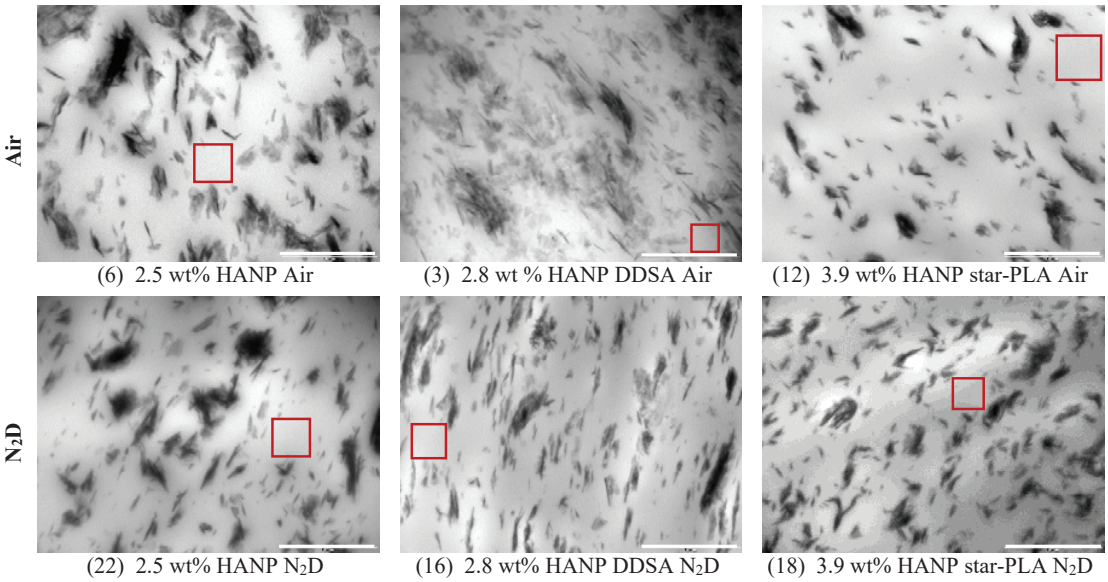

FIGURE 3. TEM images obtained with TEM FEI at x 26,500 magnification, scale bar 1 µm. All nanocomposites with nominal loading of 2.5 wt% HANP (plus coating) compounded in Air: (3), (6), (12) and in N_2D: (16), (18), (22). Numbers correspond to conditions in Table 1.

Figure 4 shows measurements of M_v as a function of τ_w at 15 min for all materials from Table 1, separated by processing gas. The gradient for both linear regressions is similar, which confirms a comparable trend. The close correlation of all the results indicates that τ_w is principally a function of M_v and that the presence of the nanoparticles does not have a significant effect on the polymer viscosity. The only significant exceptions to this appear to be the (2) 4.9 wt% HANP is-PLA8 and (3) 2.8 wt% HANP DDSA specimens. This could suggest improved dispersion in these materials, which will be studied in greater detail in future research.

Materials with the same nominal loading of HANP have higher M_v and τ_w for compounding in N_2D than in Air, demonstrating a clear benefit of N_2D in terms of preserving M_v during processing, e.g. 3.9 wt% HANP star-PLA: (18) in N_2D and (12) in Air. Additionally, decreased M_v and τ_w can be observed in N_2D for coated HANP with 5 wt% nominal loading compared with 2.5 wt%, e.g. HANP is-PLA24: (7) 11.1 wt% and (19) 5.6 wt%.

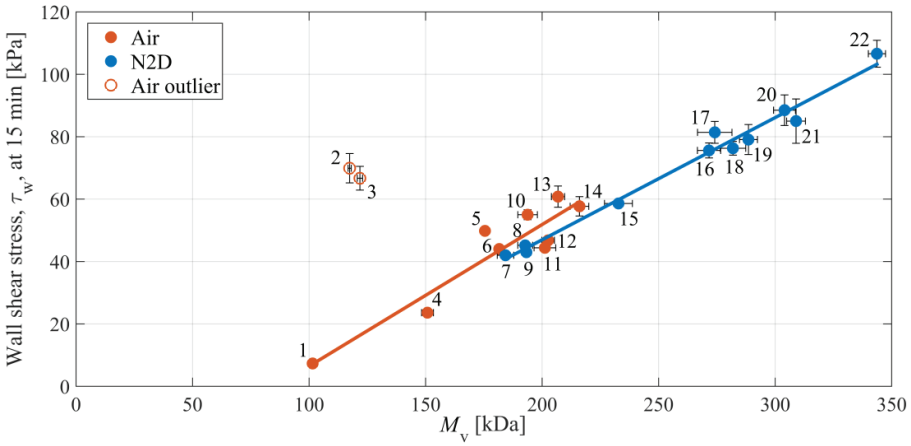

FIGURE 4. M_v for PLDLLA and nanocomposites after 15 min recirculation in the MiniLab extruder in Air and N_2D versus τ_w at 15 min. Linear regression for Air excludes (2) and (3) (4.9 wt% HANP is-PLA8 and 2.8 wt% HANP DDSA respectively).

No substantial improvements in the initial mechanical properties were seen when compounding in N_2D as compared to Air, despite increased M_v. However, increased molecular weight would improve material response during application within the body, where the fall in mechanical strength caused by degradation will be delayed in the manufactured products.

The most significant difference in the mechanical performance was for the 5 wt% HANP, where the Air extruded and IM specimen presented a 33 % increase compared to its N_2D extruded counterpart. All of the other specimens that were tested ranged from 84 MPa to 100 MPa, identifying the significance of the result of the 5 wt% HANP. It is possible that the injection moulding procedure provided additional shear during the manufacture of the specimens, allowing a superior exfoliation to be obtained, enhanced with the presence of the larger quantity of HANP. This effect allows for the improved mechanical properties seen with IM to outweigh the possible loss that would be seen due to the significant loss in molar mass of these specimens. Although the initial properties of this composite are high, the low molecular weight will cause rapid degradation during application. Further work is being undertaken to determine the influence of IM, where the use of a N_2D atmosphere will provide the improved molar mass required for application.

CONCLUSIONS

The effectiveness of novel tailored dispersants, when coated onto HANP, and nanoparticle morphology was investigated during and after compounding over ambient air and dried bottled N_2. Preliminary findings show that drying the N_2 is essential to maintain high molecular weight, which in turn yields high wall shear stress during compounding. The most significant improvement in M_v was observed when the HANP was dried at a high temperature. This is believed to remove any remaining water from the PLDLLA during processing, significantly reducing the effect of the depolymerisation ordinarily taking place at the compounding temperatures. Although the mechanical properties of the nanocomposites are not significantly affected by the moisture content, the more limited drop in molar mass is likely to play a significant role once these materials experience hydrolytic degradation during application within the body.

Preliminary TEM image analysis was carried out with a semi-quantitative approach, and revealed superior dispersion in 2.8 wt% HANP DDSA in Air when compared to other nanocomposites. This will be studied in greater detail in future research and verified with microCT measurements.

ACKNOWLEDGMENTS

This work was supported by grant EP/J017272/1 from the UK Engineering and Physical Sciences Research Council (EPSRC), and by a travel grant - Andrew Carnegie Research Fund from Institute of Materials, Minerals and Mining enabling attendance at the conference. Data created in support of this research is openly available at http://dx.doi.org/10.17639/nott.43.

REFERENCES

1. S. Bose, M. Roy & A. Bandyopadhyay, Trends in Biotechnology, 30, 546-554 (2012).
2. S. I. J. Wilberforce, C. E. Finlayson, S. M. Best & R. E. Cameron, Polymer, 52, 2883-2890 (2011).
3. M. M. Tomczynska, G. Y. H. Choong, D. S. A. De Focatiis, D. M. Grant and A. J. Parsons (in press) "Compounding and rheometry of PLA nanocomposites with coated and uncoated hydroxyapatite nanoplatelets". AIP, PPS2015 Graz Conference Proceedings.
4. G. Y. H. Choong, A. J. Parsons, D. M. Grant & D. S. A. De Focatiis, "Rheological techniques for determining degradation of polylactic acid in bioresorbable medical polymer systems", PPS Conference Proceedings 30, Polymer Processing Society, Cleveland, Ohio, 2014.
5. E. Lester, S. V. Y. Tang, A. Khlobystov, V. L. Rose, L. Buttery & C. J. Roberts, CrystEngComm, 15, 3256-3260 (2013).
6. E. Lester & B. Azzopardi (2005) Counter Current Mixing Device, Patent No. W/O 2005077505. Available at: http://www.google.com/patents/WO2005077505A2 [Accessed 30 March 2016]
7. E. Lester (2010) Hydroxyapatite material and methods of production, Patent No. W/O 2010122354. Available at: http://google.com/patents/WO2010122354A1 [Accessed 30 March 2016].
8. F. Hild, K. Walton, M. Gimeno Fabra, E. Lester & D. Irvine, "Continuous, Single Stage Synthesis of Dispersant Included Nanoparticles", NanoBioTech-Montreux Conference, Montreux, Switzerland, 2014.
9. M. Gimeno-Fabra, F. Hild, P. Dunne, K. Walton, D. Grant, D. J. Irvine & E. Lester, CrystEngComm, 17, 6175-6182 (2015).
10. O. Dechy-Cabaret, B. Martin-Vaca & D. Bourissou, Chem Rev, 104, 6147-76 (2004).
11. L. T. Lim, R. Auras & M. Rubino, Progress in Polymer Science, 33, 820-852 (2008).
12. J. R. Dorgan, J. Janzen, D. M. Knauss, S. B. Hait, B. R. Limoges & M. H. Hutchinson, Journal of Polymer Science Part B: Polymer Physics, 43, 3100-3111 (2005).
13. H. S. Khare & D. L. Burris, Polymer, 51, 719-729 (2010).